International Journal of Scientific and Technological Research
ISSN 2422-8702 (Online)
Vol 2, No.1, 2016

Numerical Investigation to Enhance Heat Transfer in a Circular Tube with Nozzles Formed Sinusoidal Geometry

Toygun Dagdevir (Corresponding author)
Department of Mechanical Engineering, Erciyes University, Kayseri, Turkey
E-mail: toygun@erciyes.edu.tr

Orhan Keklikcioglu
Department of Mechanical Engineering, Erciyes University, Kayseri, Turkey

Veysel Ozceyhan
Department of Mechanical Engineering, Erciyes University, Kayseri, Turkey

Abstract

This paper presents the effect of formed sinusoidal conical-nozzle turbulators which are embedded in a circular tube on heat transfer and friction characteristic on a uniform heat-flux applied tube. In this study, a numerical investigation was conducted to analyze heat transfer, friction characteristic and thermo-hydraulic performance by using two-dimensional axisymmetric geometry. An experimental study was used to validate numerical solution methodology and, was ensured a good agreement Nu (average Nusselt Number) and f (average friction factor). k-ε RNG turbulence model was fixed on to simulate turbulent airflow throughout the tube fitted formed sinusoidal conical-nozzles for nine different Reynolds numbers ranges from 8000 to 24000. Grid independence was ensured with three different grid models by getting less than 1% variation on average Nusselt number and average friction factor value. Twelve different configurations between amplitudes and periods were employed to introduce the effect of different geometry on thermo-hydraulic performance. Results show that amplitude and period values are of rather effects on increasing turbulent near the nozzles, and that caused to increase both increasing of heat transfer and friction factor. As a result, the highest thermo-hydraulic performance is obtained for type-11 model which is amplitude of 2 mm and period of 2.5.

Keywords: Heat transfer enhancement, friction factor, turbulent flow, sinusoidal nozzle.

1. Introduction

Energy plays a key role for development, industrial, economic, military, farming and social fields. All developed countries have enough energy sources (inclusive renewable or nuclear energy) or good energy politics. Energy requirements increase with growth of population, transportation, industrialization and global warming day by day. Because of population, global warming, consuming fossil fuels and so increasing fuel prices, investigations of augmentation of energy efficiency are most important and common subjects that are minimizing the energy costs. Within this scope, enhanced methods in heat transfer have a considerable place. Forced convection heat transfer is a common and important subject in many engineering applications such as nuclear energy, building heating, solar energy and cooling of some electronic components. However, needed pump power increases due to high friction, as forced convection heat transfer increases. Designs of a these systems that are used for heating or cooling must be considered in terms of efficiency, whether it can be employed and profitable or not.

Researchers who are interested in heat transfer enhancement area have conducted many studies on air heater. These studies are relevant as experimental or numerical (for saving time and cost) by validating experimental experiences. Rainieri et al. [1] experimentally investigated thermal performances of corrugated wall tubes employed in a broad variety of industrial applications in order to intensify the

convective heat transfer. They examined that both axial symmetrical and helical corrugations with four different pitch values for low Re numbers (90-800). The comparison between the tubes having the helical and the axial symmetrical corrugation pointed out a stronger ability of the transverse corrugation in enhancing the rate of heat transfer, by promoting a transition to the turbulent flow. Though, the spiral corrugation may be preferable in comparison with the transverse one, it can be easily fabricated on a large scale. In another experimental study, Bopche et al. [2] carried out the heat transfer and frictional characteristic by using artificially roughened U-shaped turbulator on the absorber surface of an air heater. Their study was related with various ratio of turbulator height to duct hydraulic mean diameter and turbulator pitch to height ratio ranging the Reynolds number from 3800 to 18000. They concluded that with comparing to the smooth duct, the turbulator roughened duct enhanced the heat transfer and friction factor by 2.82 and 3.72 times, respectively. Another investigator team, Eimsa-ard et al., [3] experimentally examined the effect of V-nozzle turbulators fitted in a circular tube on heat transfer, friction factor and enhancement efficiency. They have supplied increase on both heat transfer and friction factor, but also enhancement efficiency came out above 1 times as compared smooth tube. Similarly, Promvonge et al. [4] conducted to enhance heat transfer on a lot of different models and configurations for Reynolds numbers 8000-18000. They concluded that maximum enhancement of heat transfer rate over the corresponding smooth tube were found to be about 2.94 times for 2.0 of pitch ratio.

A lot of numerical studies were carried out about to enhance heat transfer. They were proposed to enhance heat transfer by changing cross-sectional area, added a lot of roughness types [5, 6, 7, 8, 9, 10]. Yadav et al. [11] were investigated heat transfer and friction factor on circular transverse wire rib roughness on the absorber plate of solar air heater. Their study is at Reynolds number ranges from 3500 to 18000 and they used the Renormalization-group (RNG) k-ε as turbulence model. They concluded that the circular transverse wire rib roughness with P/e=10.71 and e/D=0.042 supplied the optimal thermo-hydraulic performance value which can be employed. Yadav et al. [12] have investigated to see that effect of another type of solar air heater which is roughened square sectioned transverse rib. They worked out the study at same Reynolds number ranges as cited above. They concluded that the effect of square rib having P/e=10.71 and e/D=0.042 is maximum for thermo-hydraulic performance value. Ozceyhan et al. numerically investigated the heat transfer enhancement in a tube using circular cross sectional rings separated from wall. Their study was performed at Reynolds number ranges from 4475 to 43725. They concluded that the highest enhancement of 18% was succeeded for Reynolds number of 15600 [13].

2. Method

2.1. Validation of Numerical Methodology

Numerical solutions (especially CFDs) need to support with experimental results, in order to get grid independence and select a turbulent model. Otherwise, the numerical solution methodologies cannot be ensured. For this purpose, an experimental study carried out by Promvonge et al. was used for validating numerical solution [4]. They investigated that the effect of insertions of conical nozzle (C-nozzle) with different pitch ratios (PR) on heat transfers, friction factor and enhancement efficiency, in Reynolds number ranges from 8000 to 18000. A diagram of experimental setup is illustrated in Fig. 1. As depicted in Fig. 1, the test-tube section was made of copper having inner diameter of 47.5 mm (D), outer diameter (D_o) of 50.5 mm, length of 1250 mm (L) and thickness (t) of 1.5 mm. The tube was heated continually to provide uniform heat flux boundary condition by using flexible electrical wire. The outer surface of test-tube was insulated to minimize convection and radiation heat losses.

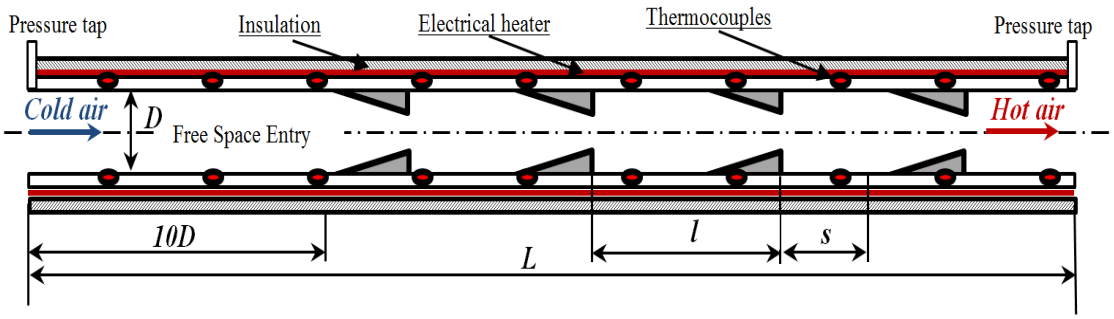

a) Experimental setup

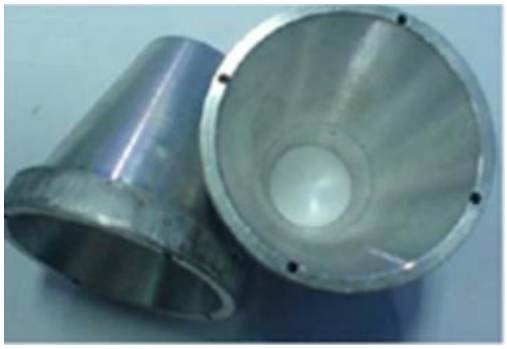

b) Used C-nozzles in the experimental setup

Figure 1. Experimental setup and C-nozzles used components in the study [4]

Validated experimental configuration is that C-nozzle is placed with pitch ratio 2.0 (l = 95 mm, s = 47.5 mm). Relationships between experimental and present study for Nu number and friction factor are given in Fig. 2 and Fig. 3, respectively. There are good agreement on both Nu and friction factor between numerical solution and experimental results.

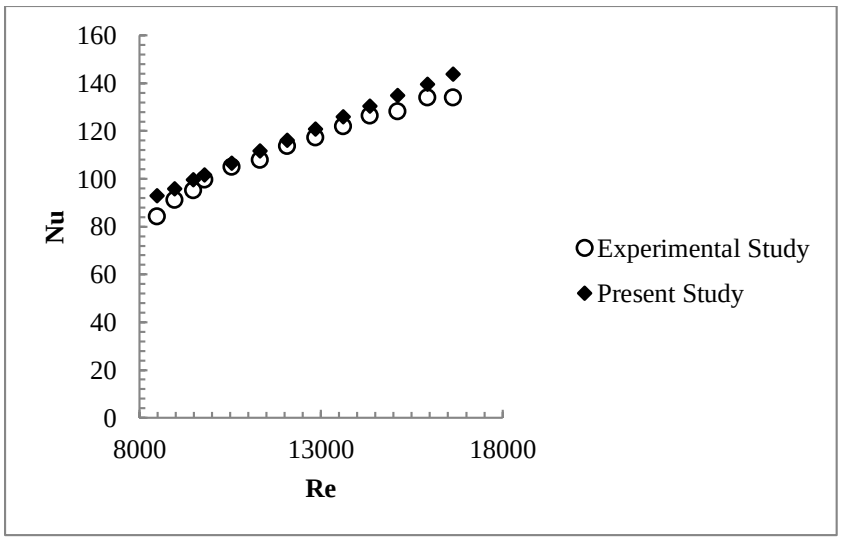

Figure 2. Nusselt number versus Reynolds number for experimental and numerical study

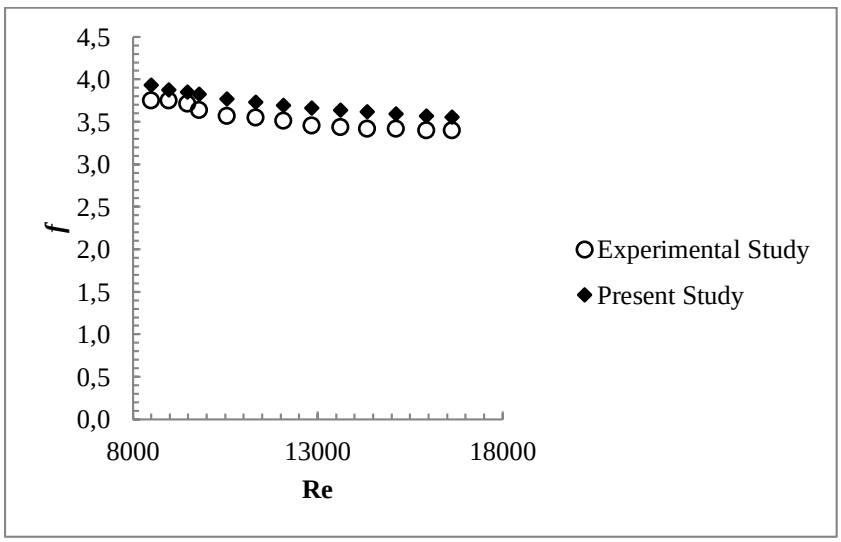

Figure 3. Friction factor versus Reynolds number experimental and numerical study

2.2. Cfd Simulation

CFD (Computational Fluid Dynamics) simulations have been commonly used to predict, solve and analyze the problems which involve fluid flows, by using equations and algorithms of fluid mechanics. Critical investigations on air heater have been carried out with developing the computers, software and advanced numerical algorithms. The advantage of CFD simulations are to optimize components of models with shorter time and cheaper than experiments.

2.2.1. Solution method

Ansys Fluent is a CFD program that simulates fluid flow and heat transfer for complex geometries. It has been using the finite-volume method to solve the essential equations of momentum, continuity, energy and turbulent. k-ε, renormalization-group (RNG) turbulence model was employed to simulate turbulent flow throughout the tube. These equations are following,

Continuity equation:

$$\frac{\partial}{\partial x_i}(\rho u_i) = 0 \tag{1}$$

Momentum equation:

$$\frac{\partial}{\partial x_i}(\rho u_i u_j) = -\frac{\partial P}{\partial x_i} + \frac{\partial}{\partial x_j}\left[\mu\left(\frac{\partial u_i}{\partial x_j} + \frac{\partial u_j}{\partial x_i}\right)\right] + \frac{\partial}{\partial x_j}\left(-\rho\overline{u_i' u_j'}\right) \tag{2}$$

Energy equation:

$$\frac{\partial}{\partial x_i}(\rho u_i T) = \frac{\partial}{\partial x_j}\left((\Gamma + \Gamma_t)\frac{\partial T}{\partial x_j}\right) \tag{3}$$

Where Γ and Γ_t are molecular thermal diffusivity and turbulent thermal diffusivity, respectively and are given by

$$\Gamma = {}^{\mu}/_{Pr} \qquad \text{and} \qquad \Gamma_t = {}^{\mu_t}/_{Pr_t} \tag{4}$$

The Reynolds-averaged approach to turbulence modeling requires that the Reynolds stresses, $-\rho\overline{u_i' u_j'}$ in Eq (2) needs to be modeled. The turbulent viscosity term μ_t is to be computed from an appropriate turbulence model. The expression for the turbulent viscosity is given as

$$\mu_t = \rho C_\mu \frac{k^2}{\varepsilon} \tag{5}$$

The modeled equation of the TKE, k is written as:

$$\frac{\partial}{\partial x_i}(\rho\varepsilon u_i) = \frac{\partial}{\partial x_j}\left[\left(\mu + \frac{\mu_t}{\sigma_k}\right)\frac{\partial k}{\partial x_j}\right] + G_k - \rho\varepsilon \tag{6}$$

Similarly the dissipation rate of TKE, ε is given by the following equation:

$$\frac{\partial}{\partial x_i}(\rho\varepsilon u_i) = \frac{\partial}{\partial x_j}\left[\left(\mu + \frac{\mu_t}{\sigma_\varepsilon}\right)\frac{\partial \varepsilon}{\partial x_j}\right] + C_{1\varepsilon}\frac{\varepsilon}{k}G_k - C_{2\varepsilon}\rho\frac{\varepsilon^2}{k} \tag{7}$$

Where G_k is the rate of generation of the TKE, while ρ_ε is its destruction rate. G_k is written as:

$$G_k = -\rho\overline{u_i' u_j'}\frac{\partial u_i}{\partial x_j} \tag{8}$$

The boundary values for the turbulent quantities near the wall are specified with the enhanced wall treatment method. C_μ=0.09, $C_{1\varepsilon}$=1.44, $C_{2\varepsilon}$=1.92, σ_k=1.0, σ_ε=1.3 and Pr_t=0.9 are chosen to be empirical constants in the turbulence transport equations [14].

Ansys Fluent 14.5 was used to solve these equations in steady regime. Grid structure was generated by using Gambit 4.4.2 and then meshed model was exported to Fluent. A pressure based, double-precision

solver was selected to solve the solution. Semi Implicit Method for Pressure Linked Equations (SIMPLE) was employed to couple the pressure and velocity. Fluent uses a point implicit (Gauss-seidel) linear equation solver in conjunction with an algebraic multigrid method [15]. Second order upwind discretization schemes were chosen on all the transport equations. The convergence criteria were assumed 10^{-6} for continuity, k, ε, x-y velocity and energy. The values of pressure drop (ΔP) and temperature difference were acquired from surface integrals in Fluent.
Reynolds number (Re), Nusselt number (Nu), friction factor (f) and thermo-hydraulic performance (THP) are non-dimensional parameters used in the present study. Reynolds number is calculated as:

$$Re = \frac{\rho DV}{\mu} \tag{9}$$

Where ρ is density, D is hydraulic diameter, V is velocity, μ is dynamic viscosity.
Average Nusselt number and heat convection coefficient (h):

$$Nu = \frac{hD}{k} \tag{10}$$

$$h = \frac{q}{T_w - T_b} \tag{11}$$

Where q is constant heat flux, T_w temperature of wall and T_b is bulk temperature
Average friction factor:

$$f = \frac{\Delta P}{\frac{1}{2}\rho\frac{L}{D}V^2} \tag{12}$$

For smooth tube, Nusselt number is calculated with Gnielinski equation (10) is valid for 2300<Re<5x106, 0.5<Pr<2000 and L/D>10 [16].

$$\mathrm{Nu_s} = \frac{\left(\frac{f}{8}\right)(\mathrm{Re_D} - 1000)\mathrm{Pr}}{1 + 12.7\left(\frac{f}{8}\right)^{\frac{1}{2}}(\mathrm{Pr}^{\frac{2}{3}} - 1)} \tag{13}$$

For smooth tube, friction factor was calculated and compared with the Darcy friction correlation given by Blasius which is presented as Eq. (11) from White [17].

$$f = 0.316Re^{-0.25} \tag{14}$$

Thermo-hydraulic performance parameter is calculated as:

$$\mathrm{THP} = \frac{\left(\frac{\mathrm{Nu_c}}{\mathrm{Nu_s}}\right)}{(f_c/f_s)^{1/3}} \tag{15}$$

Where "c" subscript is for study with C-nozzles; "s" subscript is for smooth tube.
Present study was carried out on different twelve different configurations of C-nozzle formed sinusoidal geometry, for nine Reynolds numbers. Some assumptions were accepted for the numerical solution:

- The flow is steady, fully developed, turbulent and axisymmetric 2D
- The used fluid (air) is assumed ideal gas and temperature of velocity inlet is 300 K
- No-slip boundary condition is appointed to the walls that contact with fluid
- Radiation, heat transfer and other heat losses are assumed negligible.

2.2.2. Grid Independence

Quad paves grid distribution in x and y directions have been generated for fluid and solid faces by using Gambit 2.4.4. To provide grid independence, three different grid models were run. The numbers of cells of them are 264,600, 532442 and 1,013,480. It is found that after 532,442 cells, further increase in cells has negligible effects on the results (less than 1%). Different grid models can be seen in Fig. 4 and all of them have boundary layer mesh to solve viscous effect of flow (Fig. 5). y^+ has been using commonly in CFD studies to explain grid sensibility near the wall. It is preferred that $0<y^+<5$ near the walls in contact with the flow. In this study y+ value is nearby two, and viscous effects are not passed over [18].

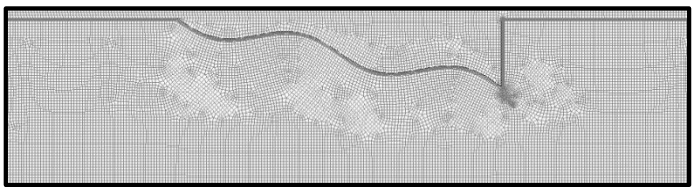

a) Grid model-1, cell number is 264,000

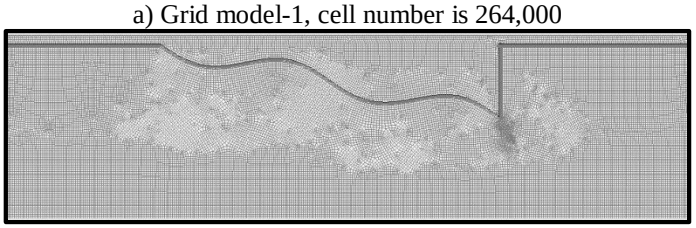

b) Grid model-2, cell number is 532,442

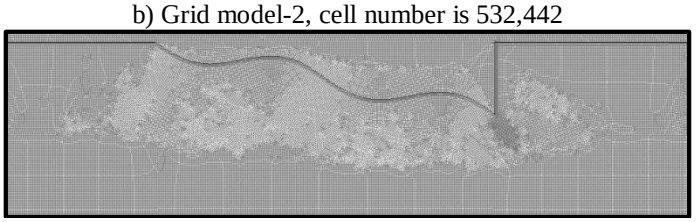

c) Grid model-3, cell number is 1,013,480

Figure 4. Grid models around a sinusoidal C-nozzle

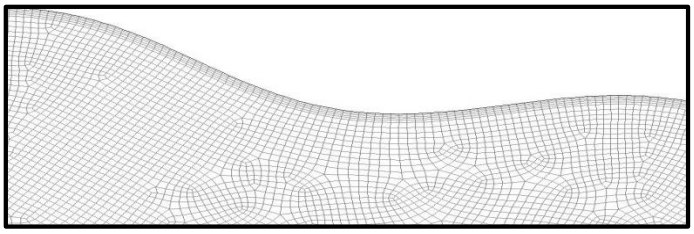

Figure 5. Boundary mesh on the wall

2.2.3 Boundary Conditions

Determining boundary conditions are so important to be able to get a good agreement with experimental results. Numerical solutions can sometimes reach a deadlock due to wrong or lack of boundary condition. In Fig. 6 computational domain is depicted for the tube embedded C-nozzle formed sinusoidal geometry. Due to reduce cell number and solution time, model was chosen as 2D axisymmetric. Uniform air velocity is applied as "Velocity inlet", and out is defined as "Pressure outlet". The material of outer tube and C-nozzles were selected from copper and aluminum, respectively.

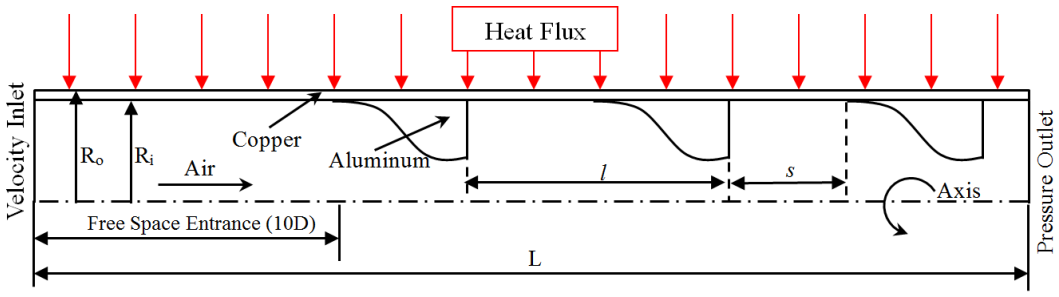

Figure 6. Computational domain for the tube embedded C-nozzle formed sinusoidal geometry

The values of the thermo-physical properties of air are constant for 300 K. Velocity magnitude has been calculated based on Reynolds number. At the exit, pressure outlet boundary condition is specified with gauge pressure of 0 Pa. At the inlet velocity inlet is normal to boundary and uniform. Flow characteristic has been provided as fully-developed with free-space entrance, and boundary layer velocity profile can

be seen in Fig. 7. The turbulence intensity (I) has been estimated fully-developed tube flow from Eq.12, as Yadav et al. used [5]. Uniform heat flux (constant q=1000 W/m^2) has been applied outer surface of the tube. The walls in contact with the fluid have no-slip boundary condition. Material properties and boundary conditions of the present study are summarized in Table 1 and Table 2.

$$I = 0.16Re^{-1/8} \quad (16)$$

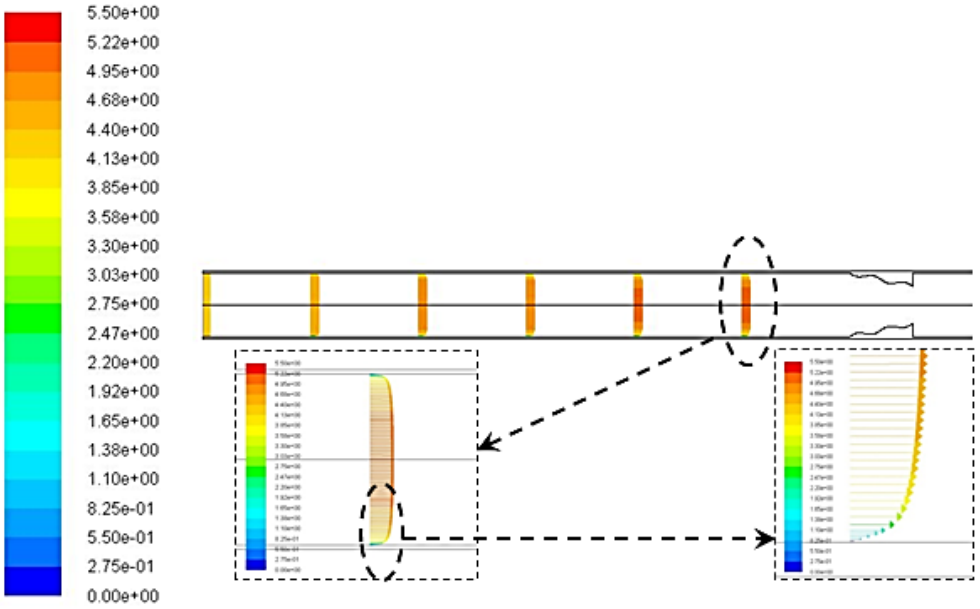

Figure 7. Velocity vector of fully-developed flow and boundary layer velocity profile

Table 1. Properties of materials used in numerical analyze

	Air	Copper	Aluminum
Density, "ρ" [kg/m^3]	Ideal gas	8978.0	2719.0
Thermal conductivity, "k" [W/mK]	0.0242	387.6	202.4
Specific heat, "Cp" [j/kgK]	1006.43	381.0	871.0
Viscosity, "μ" [kg/ms]	1.7894E-05	-	-

Table 2. Boundary conditions in numerical analyze

Heat flux (constant), "q" [W/m^2]	1000
Velocity magnitude, "V" [m/s]	Calculated based on Re
Gauge pressure [Pa]	0
Gravity, "g" [m/s^2]	9.807

As summarized in Table 3 and Fig. 8, C-nozzles were placed with four periods and three amplitude values (A=1, 2 and 3 mm) after free space entrance, for each numerical solution. Horizontal length of sinusoidal geometry (λ) is 60 mm, constantly, and end and throat diameter are 60 mm and 37.50 mm, respectively. Because the length of C-nozzle is constant, each period type has different wave length.

Table 3. Geometric features of investigated types

Type	***1***	***2***	***3***	***4***	***5***	***6***	***7***	***8***	***9***	***10***	***11***	***12***
Period	1	1	1	1.5	1.5	1.5	2	2	2	2.5	2.5	2.5
Wave length [mm]	60	60	60	40	40	40	30	30	30	24	24	24
Amplitude [mm]	1	2	3	1	2	3	1	2	3	1	2	3

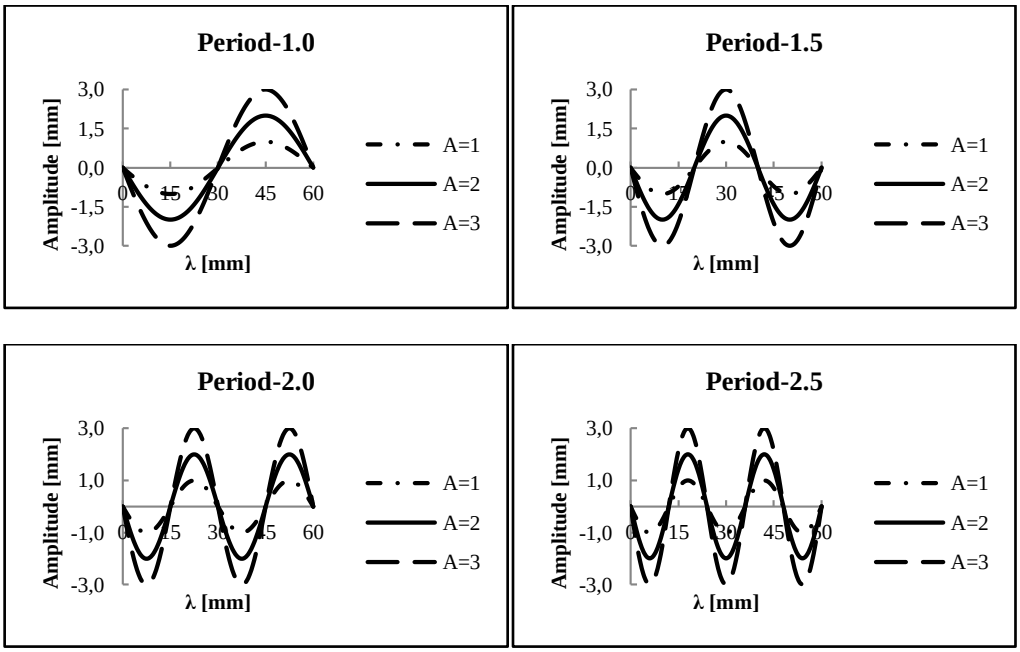

Figure 8. Configurations based on period and amplitude values

3. Results and Discussion

In this study, a different computational model from literature was investigated on heat transfer and friction factor. C-nozzles have been employed to enhance turbulence; consequently heat transfer. Twelve different configurations have been investigated to introduce variations on Nusselt number and friction factor. The parameters in these configurations are three amplitude and four period values on sinusoidal form.

3.1. Average Heat Transfer

The present numerical results on average heat transfer characteristic for twelve different types and smooth tube are presented in the form of average Nusselt number in Fig. 9. Average Nusselt number of sinusoidal C-nozzle with respect to the smooth tube with increasing values of Reynolds number in all cases, as expected.

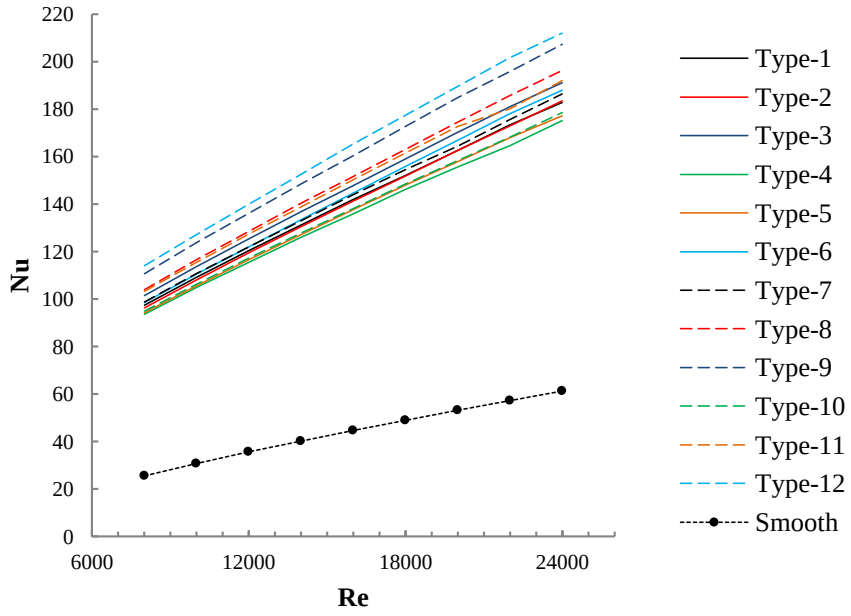

Figure 9. Variation of average Nusselt number versus Reynolds number for twelve configurations and smooth tube

Numerical results clearly show that increase in period and amplitude value increases the heat transfer. The reason for increasing in Nusselt number is that turbulent occurs and especially intensifies exit of the C-nozzles. The effect of period number and that of amplitude on Nusselt number are illustrated in Fig 10 and Fig 11, respectively.

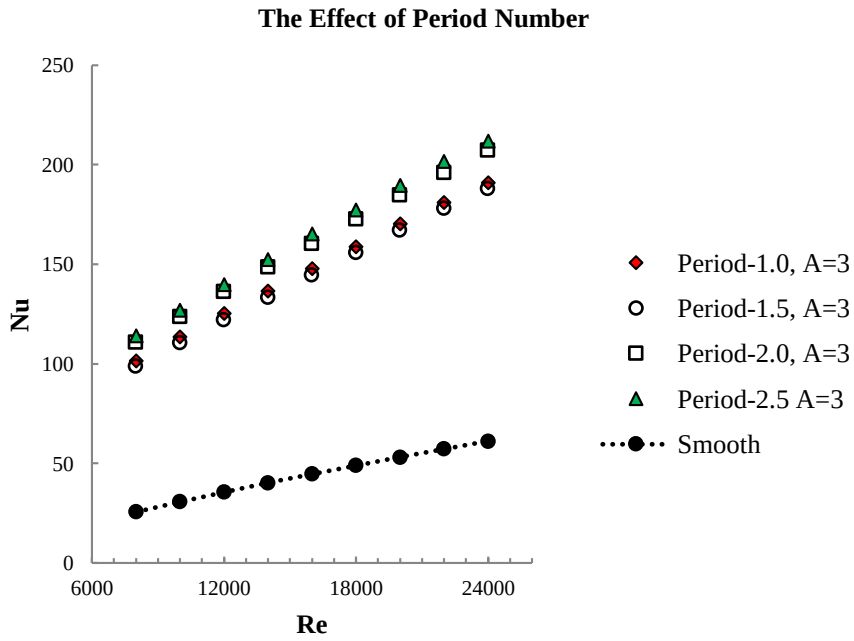

Figure 10. The effect of period number on Nusselt number for constant amplitude of 3mm.

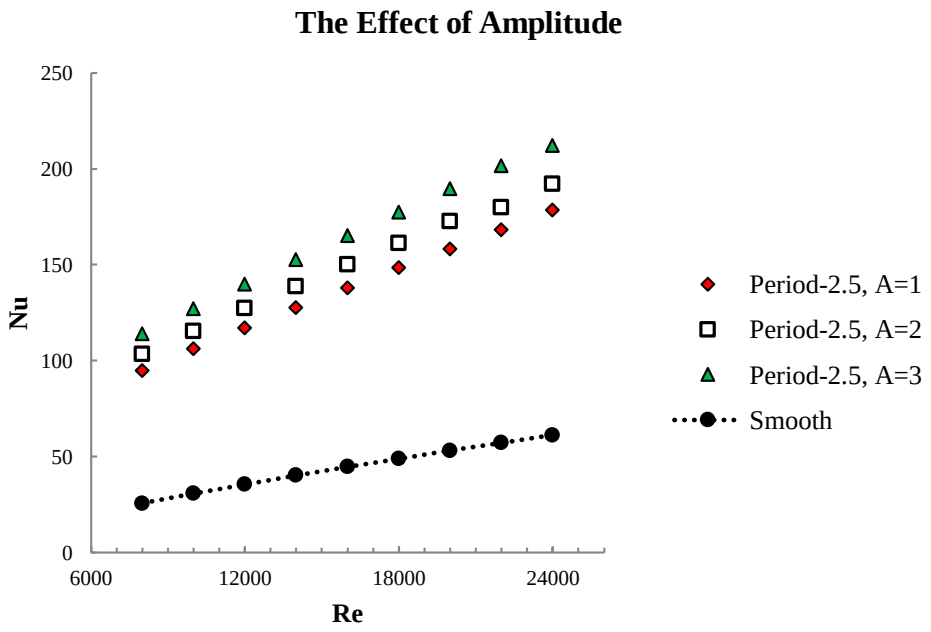

Figure 11. The effect of amplitude value on Nusselt number for constant period-2.5.

Maximum average Nu number has been obtained on Type-12 which is 2.5-period, amplitude of 3 mm at Reynolds number of 24000. It is clear that the average Nusselt number is enhanced when rise period numbers and amplitude values due to increasing surface area and turbulence.

3.2. Average Friction Factor

As shown in Fig. 12, 13 and 14, friction factor tends to fall with increasing Reynolds number. It is clear that sinusoidal surface increase the friction since it prevents the flow suddenly. The effect of period number and amplitude on friction factor illustrate in Fig 13 and 14, respectively.

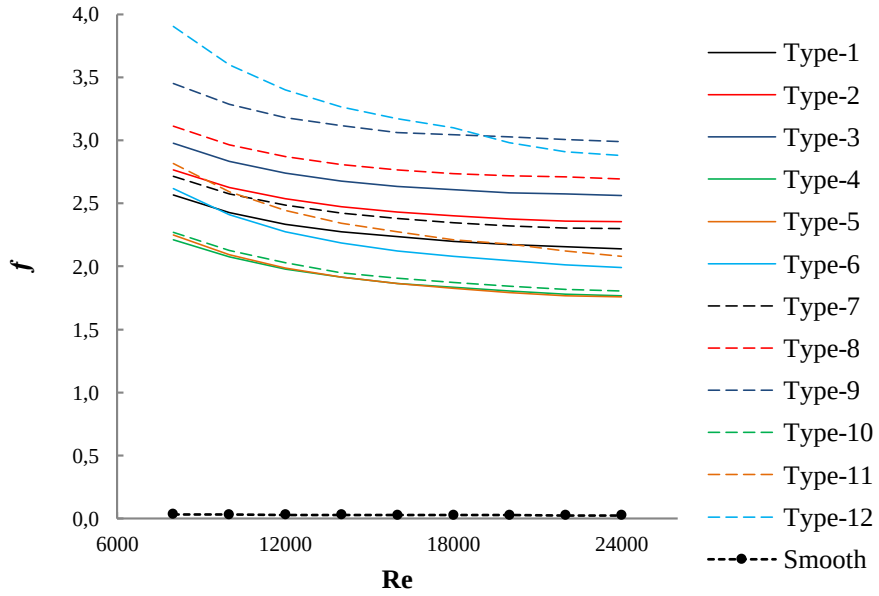

Figure 12. Variation of average friction factor with Reynolds number for different twelve types and smooth tube

On increased amplitude value, friction factor increases for constant period number, as well. Yet, when period number increases, variation of friction factor does not occur similarly. Cause of this turbulence effect differently consists in terms of period number. Minimum friction factor has been obtained on

Type-4 which is 1.5 period, amplitude is 1mm at Reynolds number of 24000, as can be seen in Fig 11. Fig 15 shows that embedded sinusoidal C-nozzles in the tube increase the velocity value at each exit of nozzle. The velocity is gradually increasing and pressure drop occurs much more. Due to these reasons, the friction factor in embedded sinusoidal C-nozzle is much more than the smooth tube. This is not a preferred situation that is increased friction because more pump power is required. So, designers have to consider what system requires.

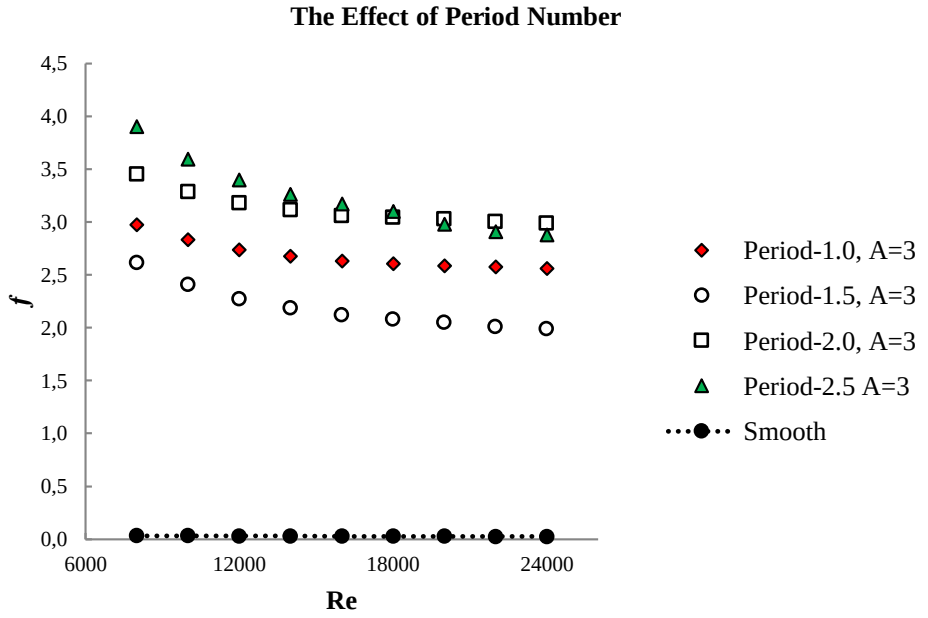

Figure 13. The effect of period number on friction factor for constant amplitude of 3mm.

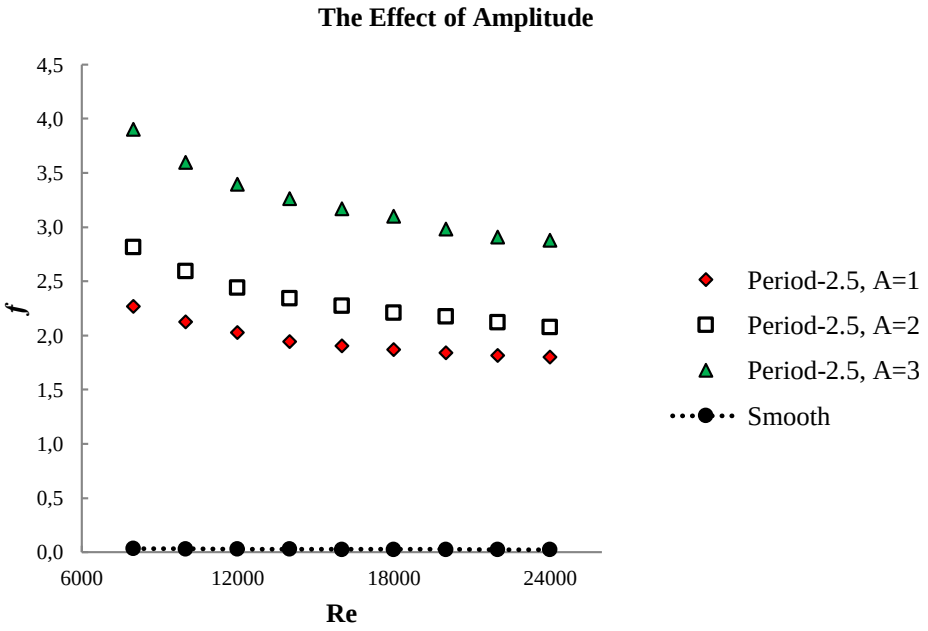

Figure 14. The effect of amplitude number on friction factor for constant period-2.5.

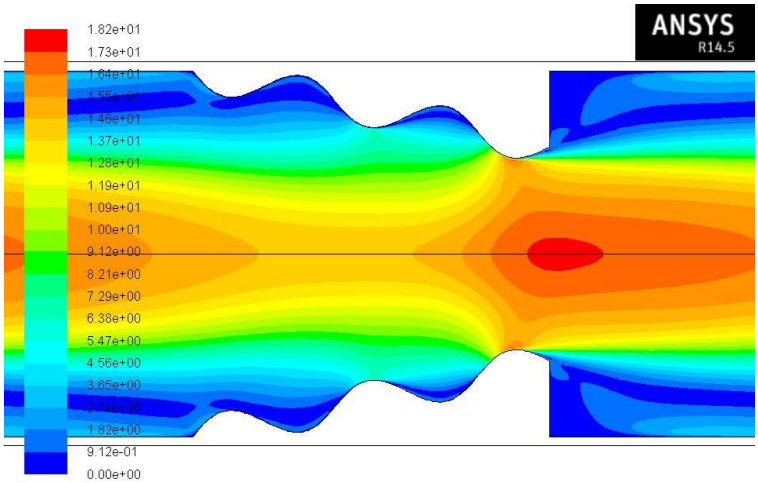

Figure 15. Contour of velocity magnitude at Re number of 16000 for Type-12.

Increasing amplitude and period values cause to increase both heat transfer and friction factor. In Fig. 16, thermo-hydraulic performance criteria by using Nu_c, f_c, Nu_s and f_s is defined as equation 10 is less than smooth tube. Because of first reason of that, friction factor is higher than smooth tube.

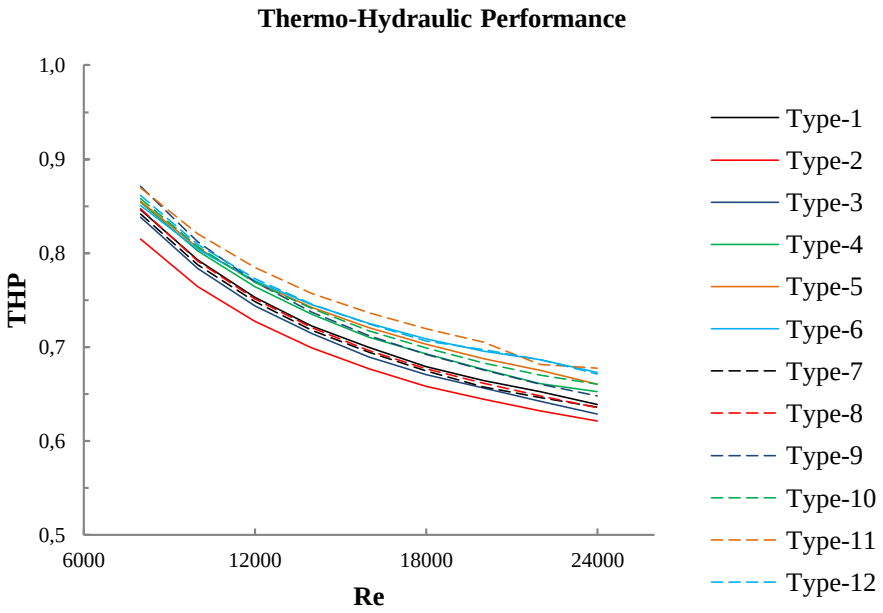

Figure 16. Thermo-hydraulic performance with Reynolds number for different twelve types

Fig. 17 shows the contour of turbulence intensity at Reynolds number of 16000 for Type-12. The peak value of turbulence intensity can be seen at latest wave of exit of C-nozzle. Type-4, 5, 6, 10 and 11 are same turbulent pattern due to having half tide geometry. However, Type-1, 2, 3, 7, 8 and 9 have full tide geometry and results show that less turbulence occurs exit of C-nozzle, as compared between in Fig. 17 and Fig 18.

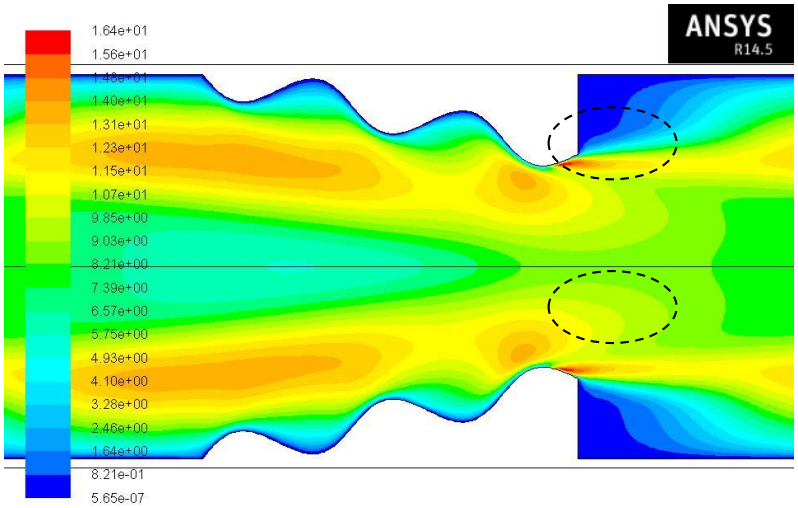

Figure 17. Countour of turbulent at Re number of 16000 for Type-12.

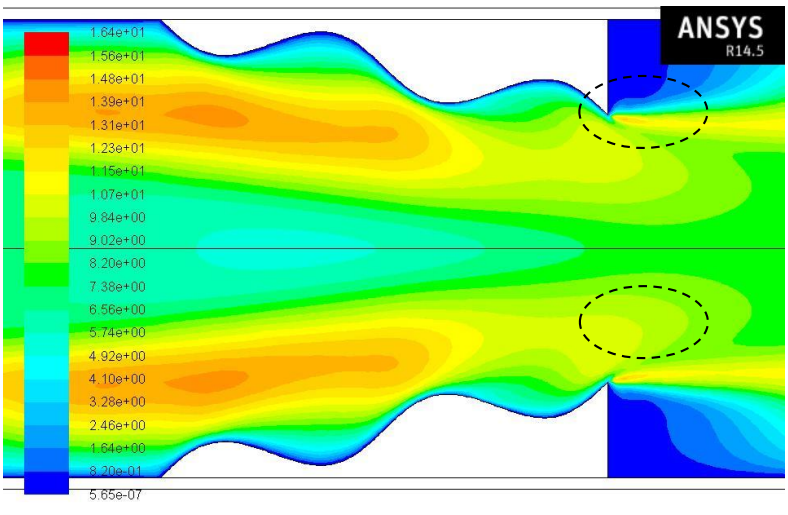

Figure 18. Contour of turbulent at Re number 16000 for Type-9

The maximum Nu number and friction factor is obtained Type-12 and the second one is Type-9. The difference between them affecting the result is turbulent near the exit of C-nozzle. This difference is increasing both heat transfer and friction.

4. Conclusion

In this study a two-dimensional axisymmetric CFD model of embedded C-nozzles formed sinusoidal geometry has been aimed to investigate the effect of wavy surface (sinusoidal form) on heat transfer and friction factor at Reynolds number ranges from 8000 to 24000. Using this approach, the study is carried out to analyze the impact of three amplitude values (A=1, 2 and 3mm) and four period values (Period-1.0, 1.5, 2.0, and 2.5). The major conclusions of this study are as following:

1-The average Nusselt number inclines to increase at the used Reynolds numbers. The maximum Nusselt number has been found on half-tide period values, like Type-12 and Type-9. Increasing amplitude values enhance the Nusselt number in same period, as well. It can be said that cause of the heat transfer enhancement in these variations is that raising the surface area which occurs convection heat transfer and rising up the turbulent near the wall.

2-The average friction factor tends to decrease as the Reynolds number increases. The major causes of that is increasing average velocity magnitude. However, drop of pressure is rise up between the inlet and

outlet of the C-nozzle. The maximum friction factor occurs for Type-12 (period-2.5, A=3 mm) as expected.

3-Increasing heat transfer and friction is an expected situation, but there is an optimal configuration. The optimal configuration is determined with thermo-hydraulic performance. Type-11 has the maximum thermo-hydraulic performance at average Reynolds numbers. However, this type is even worse than smooth tube as considered thermo-hydraulic performance. But when the heat transfer is more important, namely friction can be ignored, this study can give an opinion to interests.

References

[1] S. Rainieri, G. Pagliarini, Concevtive Heat transfer to temperature dependent property fluids in the entry region of corrugated tubes, International Journal of Heat and Mass Transfer, Vol. 45, pp. 4525-4536, 2002.

[2] S. B. Bopche, M. S. Tandale, Experimental investigations on heat transfer and frictional characteristics of a turbulator roughened solar air heater duct, International Journal of Heat and Mass Transfer, Vol. 52, pp. 2834-2848, 2009.

[3] S. Eimsa-ard, P. Promvonge, Experimental investigation of heat transfer and friction characteristics in a circular tube fitted with v-nozzle turbulators, International Communications in Heat and Mass Transfer. Vol. 33, pp. 591-600, 2006

[4] P. Promvonge, S. Eimsa-ard, Heat transfer enhancement in a tube with combined conical-nozzle inserts and swirl generator, Energy Conversion and Management, Vol. 47. pp. 2867-2882, 2006.

[5] Z. Carija, B. Frankovic, M. Percic, M. Cavrak, Heat transfer analysis of fin and tube heat exchangers with flat and louvered fin geometries, International Journal of Refrigeration, Vol. 45. pp. 160-167

, 2014.

[6] B. Lofti, M. Zeng, B. Sunden, Q. Wang, 3D numerical investigation of flow and heat transfer characteristics in smooth wavy fin-and-elliptical tube heat exchangers using new type vortex generators, Energy, Vol. 73, pp. 233-257, 2014.

[7] S. V. Patankar, Numerical heat transfer and fluid flow, Washington DC, Hemisphere, 1980.

[8] S. Kumar, R.P. Saini, CFD based performance analysis of a solar heater duct provided with artificial roughness, Renewable Energy, Vol. 34, pp. 1285-1291, 2009.

[9] Y. Varol, H. F. Oztop, A comparative numerical study on natural convection in inclined wavy and flat-plate solar collectors, Building and Environment, Vol. 43, pp. 1535-1544, 2008.

[10] A. Chaube, P. K. Sahoo, S. C. Solanki, Effect of roughness shape on heat transfer and flow friction characteristics of solar air heater with roughened absorber plate, WIT Transactions on Engineering Sciences, Vol. 53, pp. 43-51, 2006.

[11] A. S. Yadav, J. L. Bhagoria, A CFD (computational fluid dynamics) based heat transfer and fluid flow analysis of a solar air heater provided with circular transverse wire rib roughness on the absorber plate, Energy, Vol. 55, pp. 1127-1142, 2013.

[12] A. S. Yadav, J. L. Bhagoria, A numerical investigation of square sectioned transverse rib roughened solar air heater, International Journal of Thermal Sciences, Vol. 79, pp. 111-131, 2014.

[13] V. Ozceyhan, S. Gunes, O. Buyukalaca, N. Altuntop, Heat transfer enhancement in a tube using circular cross sectional rings separated from wall, Applied Energy, Vol. 85, pp. 988-1001, 2008.

[14] B. E. Launder, D. B. Spalding, Lectures in Mathematical Models of Turbulence, Academic Press, London, 1972.

[15] Fluent release6.2.16, Fluent Incorporated, 2005.

[16] S. Kakac, R. K. Shah, A.E. Bergles, Low Reynolds number flow heat exchangers, Hemisphere, Washington, 1982.

[17] F. M. White Viscous Fluid Flow, 2nd edition Mc Graw Hill, New York, 1991.

[18] M. Ariff, S. M. Salim, S. C. Cheah, Wall y+ approach for dealing with turbulent flow over a surface mounted cube: Part1-Low Reynolds number, Seventh International Conference on CFD in the Minerals and Process Industries CSIRO, Melbourne, 2009.

NOMENCLATURE

A	Amplitude, mm	Tb	Mean temperature of fluid, K
Cp	Specific heat of air, j/kg-K	s	Spacing between two nozzle, mm
D	Hydraulic diameter, mm	Ri	Radius of fluid area, mm
g	Gravity, m/s^2	Ro	Radius of copper, mm
h	Heat transfer coefficient, W/m^2-K	V	Velocity magnitude of fluid, m/s
k	Thermal conductivity of air, W/m-K	μ	Dynamic viscosity, kg/m-s
L	Length of tube, mm	ρ	Density, kg/m^3
l	Pitch, mm	ΔP	Pressure drop, Pa
q	Heat flux, W/m^2	Γ	Molecular thermal diffusivity, m^2/s
T	Air temperature, K	Γt	turbulent thermal diffusivity, m^2/s
Ty	Surface temperature of wall, K		

Dimensionless parameters

I	Turbulence intensity, dimensionless	Re	Reynolds number
Nuc	Average Nusselt number for C-nozzles	Pr	Prandtl number
Nus	Nusselt number for smooth tube	THP	Thermo-Hydraulic performance
fc	Friction factor for C-nozzles	y+	Non dimensional wall coordinate
fs	Friction factor of smooth tube		